geotechnics

MDPI

Article

Feasibility Study of Fiber-Reinforced Dredged Reservoir Sediment for Landfill Cover Applications

Rafika Lachache [1], Salim Kouloughli [1], Ana Bras [2] and Halima Belhadad [3,*]

[1] Department of Civil Engineering, Université des Frères Mentouri Constantine 1, Constantine 25000, Algeria; rafika.lachache@doc.umc.edu.dz (R.L.); salimkouloughli@umc.edu.dz (S.K.)
[2] Built Environment and Sustainable Technologies (BEST) Research Institute, Liverpool John Moores University, Byrom Street, Liverpool L3 3AF, UK; a.m.armadabras@ljmu.ac.uk
[3] Energy Physics Laboratory (EPL), Faculty of Exact Sciences, University Constantine 1, Route Ain El Bey, Constantine 25000, Algeria
* Correspondence: belhadadhalima@outlook.fr or halima.belhadad@doc.umc.edu.dz

Abstract

Dredged reservoir sediments (DRS), generated in large volumes during dam desilting operations, pose significant stockpiling and land-use challenges in Mediterranean regions. Owing to their high fines content and moderate plasticity, these sediments present potential for reuse as compacted hydraulic barrier materials. This study evaluates the feasibility of using DRS as a liner material and, for the first time, provides a direct comparative assessment of natural (wheat straw fibers, WSF) and synthetic (polypropylene fibers, PPF) reinforcement within the same sediment matrix under liner-relevant conditions. Fiber contents of 0–0.9% (by dry mass) were investigated. Mechanical and consolidation behaviors were assessed using direct shear and oedometer tests. Fiber inclusion significantly improved shear strength, with an optimal response at 0.6%. At this dosage, PPF reduced the compression index by ~50%, while WSF provided moderate but consistent improvement. Estimated hydraulic conductivity increased slightly with fiber addition but remained within the range typically reported for compacted barrier materials. FTIR analysis indicated distinct reinforcement mechanisms, with lignocellulosic interactions for WSF and mechanical bridging for PPF. These results demonstrate that DRS can be effectively valorized as liner materials, while highlighting the contrasting performance of biodegradable and synthetic fibers, with 0.6% identified as a balance between mechanical efficiency and material sustainability.

Keywords: dredged reservoir sediment; compacted clay liner; landfill cover systems; fiber-reinforced soil; wheat straw fiber; polypropylene fiber; consolidation behavior; hydraulic conductivity; geotechnical valorization

Academic Editors: Yong Sheng and Xin Huang

Received: 16 January 2026
Revised: 23 March 2026
Accepted: 24 March 2026
Published: 31 March 2026

1. Introduction

Engineered barrier systems constitute a fundamental component of modern landfill and waste containment facilities. Their primary function is to prevent the migration of leachates into surrounding soil and groundwater, thereby limiting environmental contamination. In arid and semi-arid regions, barrier performance may be further challenged by climatic factors such as desiccation, shrinkage cracking, and cyclic wetting–drying, which can increase the risk of preferential flow and contaminant migration if liner integrity is compromised [1,2]. Among barrier technologies, compacted clay liners (CCLs) remain widely adopted due to their low hydraulic conductivity, sorptive capacity, and compatibility with natural soils [3–5]. Regulatory frameworks typically require hydraulic conductivities on

the order of 10^{-9} m/s for basal liners and $\leq 10^{-7}$ m/s for final cover systems, while maintaining sufficient shear strength to ensure slope stability and controlled compressibility to prevent differential settlement and cracking [4,6].

Despite their proven performance, the use of natural clayey soils in liner construction is increasingly constrained by material availability and environmental considerations [7]. Suitable borrow materials are not always locally accessible, particularly in arid and semi-arid regions, and their extraction may lead to ecological disturbance, transport-related impacts, and increased project costs [8]. Consequently, interest has expanded toward alternative fine-grained geomaterials, including industrial by-products and reservoir dredged sediments. It is recognized, however, that dredged sediments are inherently heterogeneous materials whose composition may vary widely depending on their origin [9–11]. When characterized by a significant fines fraction and adequate plasticity, certain sediments may exhibit mechanical and hydraulic behaviors compatible with liner requirements, provided that their performance is verified against established specifications [9].

Reservoir sedimentation represents a major environmental and hydraulic challenge in Mediterranean regions, where semi-arid climatic conditions, intense watershed erosion, and highly irregular rainfall regimes accelerate siltation processes. In North Africa, dam infrastructures are experiencing particularly high sediment accumulation rates, resulting in significant losses of effective storage capacity and reduced long-term water resource availability. To counteract this decline, periodic dredging operations are implemented, generating substantial volumes of dredged dam/reservoir sediments (DDS/DRS). In Algeria alone, annual sediment deposition in reservoirs is estimated to exceed 20 million m^3 [12–14], while globally, hundreds of millions of tons of sediments are dredged each year [15].

Conventional management practices primarily involve open-air stockpiling near dam sites. This approach creates environmental constraints, occupies valuable land, and may lead to secondary impacts such as dust emissions, leachate generation, or landscape degradation, while offering limited economic or material valorization potential. Consequently, the reuse of dredged sediments has emerged as an increasingly attractive and sustainable management strategy.

Numerous studies have explored the potential incorporation of dredged sediments in civil engineering and related sectors. Reported applications include their use in road pavement structures [16–18], brick manufacturing [19], partial replacement of natural aggregates (e.g., sand substitution) [20], supplementary cementitious materials (SCMs) [21,22], self-consolidating concrete (SCC) [23], geopolymer binders [24], and even agricultural soil amendments [25]. These investigations demonstrate the technical feasibility of sediment valorization; however, most focus on structural or construction-material applications, with comparatively fewer studies addressing their use in geotechnical containment systems.

From a geotechnical perspective, DRS often exhibit high fines content, moderate plasticity, and mineralogical compositions dominated by silicates and carbonates, making them broadly comparable to clayey soils traditionally used in liner applications [4,26]. Several studies have demonstrated the technical feasibility of using dredged sediments or water treatment sludges as barrier materials [27,28] provided they undergo appropriate processing or modification.

For liner applications, mechanical stability is as critical as hydraulic performance. Low shear strength may compromise slope stability, while high compressibility can lead to differential settlement and cracking, increasing the risk of preferential flow paths. Conventional stabilization techniques, such as cement/lime [29], ashes [30] and gums [30] stabilization, can significantly improve mechanical properties but often increase permeability, carbon footprint, and cost, and may alter the chemical compatibility of the liner [12,13].

In this context, fiber reinforcement has emerged as an attractive alternative for improving the engineering behavior of fine-grained soils without fundamentally altering their mineral structure [31–33]. Unlike cementitious additives, fibers are incorporated at low dosages (typically <1% by dry mass), require no curing period, and primarily modify mechanical behavior through physical mechanisms rather than mineralogical alteration [34].

The reinforcement of soils with randomly distributed fibers has been widely studied over the past two decades. Both natural and synthetic fibers [35,36] have been shown to enhance shear strength, ductility, and resistance to crack propagation, primarily through mechanisms of fiber bridging, frictional interlock, and stress redistribution within the soil matrix.

Synthetic fibers, particularly polypropylene fibers (PPF), are characterized by high tensile strength, chemical inertness, and durability. Numerous studies have reported significant improvements in shear strength and reductions in compressibility of clayey soils reinforced with low PPF contents (typically 0.25–1.0%) [37]. In contrast, natural fibers, such as straw, coir, olive husk, or jute, offer advantages in terms of renewability, low density, and reduced environmental impact, but their hydrophilic nature and lower stiffness may influence water retention and long-term behavior [38–40].

Despite the extensive body of research on fiber-reinforced soils, most investigations have focused on strength improvement in conventional clays for embankment or pavement applications, with limited attention to liner-oriented performance criteria. In particular, comparative evaluations of natural and synthetic fibers incorporated within the same fine-grained sediment matrix under compaction and stress conditions representative of barrier systems remain scarce. The influence of fiber type and dosage on the coupled mechanical and volumetric response of sediment-based liners specifically shear strength, compressibility, and the implications for hydraulic compliance has not been systematically examined within a unified experimental framework. Furthermore, few studies attempt to relate macroscopic geotechnical behavior to microstructural evidence in sediment-derived materials.

Within this context, the present study evaluates the feasibility of using fiber-reinforced reservoir dredged sediment (DRS) as a compacted liner material for waste containment applications. The investigation focuses on sediment obtained from the Ksob Dam, M'sila, (Algeria), characterized by a high fines content and moderate plasticity, and examines reinforcement using wheat straw fibers (WSF) and polypropylene fibers (PPF) at dosages ranging from 0 to 0.9% by dry mass of sediment. The comparison is methodological and performance-driven: PPF represents a durable synthetic benchmark widely used in geotechnical practice, whereas WSF represents a locally available bio-based alternative.

The experimental program integrates direct shear testing, one-dimensional consolidation, density and porosity assessment, and Fourier Transform Infrared Spectroscopy (FTIR) to elucidate the relationships between reinforcement mechanism and engineering response. By assessing natural and synthetic fibers within the same sediment system and under liner-relevant performance criteria, the study provides a structured feasibility evaluation of sediment-based barrier materials. The contribution lies not in introducing a new reinforcement concept, but in delivering a comparative, application-oriented assessment that supports the valorization of reservoir sediments within a resource-constrained Mediterranean context.

2. Materials and Methods

2.1. Materials

2.1.1. Dredged Reservoir Sediments (DRS)

The soil investigated in this study is a dredged reservoir sediments (DRS) obtained from desilting operations at Ksob Dam, M'Sila, Algeria. A representative composite

sample (Table 1) was prepared by collecting and homogenizing five sub-samples from the storage area (Figure 1) to ensure it accurately reflects the overall composition of the stored sediments, thereby supporting its potential application in landfill liner and cover systems.

Table 1. Description of the sediment sample from the dredged storage area of Ksob Dam (M'Sila, Algeria).

Sample ID	Origin	Number of Sub-Samples	Latitude (°N)	Longitude (°E)
DRS	Dredged sediment storage area	5	35.8412	4.5721

Figure 1. Storage area of dredged sediments from Ksob Dam (M'Sila, Algeria).

Geotechnical characterization of the DRS was carried out in accordance with ISO 17892-4 [41] (particle-size distribution) (Figure 2), ISO 17892-3 [42] (density of solid particles), ISO 17892-12 [43] (Atterberg limits), and ISO 10694 [44] (organic matter content). The plasticity index (PI) was used to calculate the clay activity (CA), which provides insight into the swelling–shrinkage potential and dominant clay mineral family. The physical and geotechnical properties of the DRS are summarized in Table 2.

The microstructural features of the DRS were examined using scanning electron microscopy (SEM), revealing a dense arrangement of fine particles with irregular morphologies and interparticle contacts typical of silt–clay mixtures, as illustrated in Figure 3.

Further chemical characterization was performed using X-ray fluorescence (XRF) analysis. The chemical composition of the DRS, presented in Table 3, is dominated by SiO_2, CaO, and Al_2O_3, confirming the mineral nature of the sediment and its similarity to clayey geomaterials commonly employed in liner systems. The relatively high CaO content may further contribute to particle bonding and mechanical stability upon compaction.

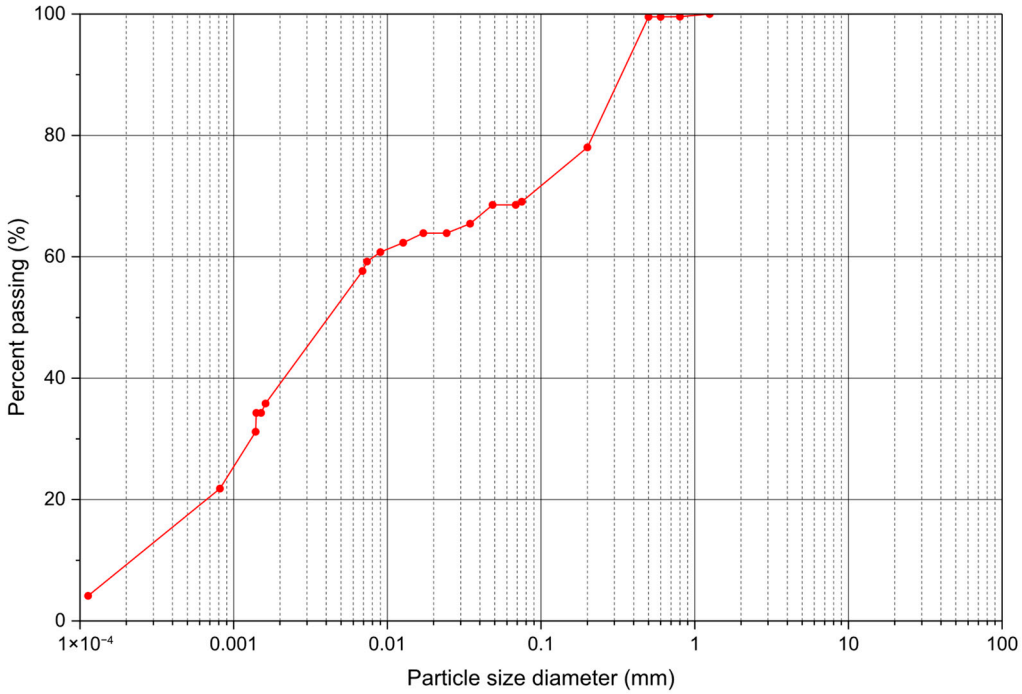

Figure 2. Particle size distribution of the dredged reservoir sediments (DRS).

Table 2. Physical and geotechnical characteristics of the dredged reservoir sediments (DRS).

Property	Value
Grain Size Distribution (%)	
Sand (%)	28.45
Silt (%)	45.17
Clay (%)	26.38
Soil Classification (USCS)	MH (**high-plasticity silt**)
Specific Gravity (Gs)	2.66
Total Specific Surface Area (cm^2/g)	157.5
Clay Activity (CA)	1.15
Organic Matter Content (%) at 450 °C	4.7
Atterberg Limits (%)	
Liquid Limit (wL)	61
Plastic Limit (wP)	31.18
Plasticity Index (PI)	29.82
Compaction Characteristics	
Optimum Water Content (%)	14.80
Maximum Dry Density (kN/m^3)	15.54

Table 3. Chemical composition of the dredged reservoir sediment (DRS)determined by XRF analysis.

	SiO_2	CaO	Al_2O_3	Fe_2O_3	MgO	K_2O	Na_2O	SO_3	Chloride	LOI
w%	41.25	18.64	12.08	4.89	1.86	1.61	0.42	0.17	0.02	18.5

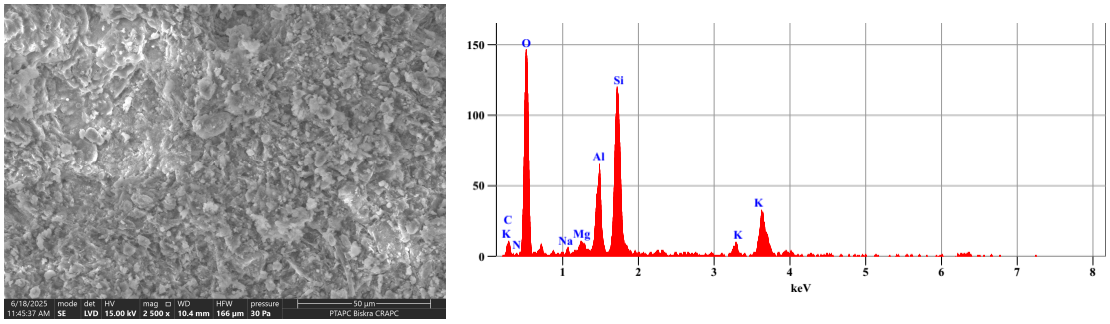

Figure 3. SEM/EDS images of the DRS used in this work.

2.1.2. Fibers: Natural and Synthetic

Two types of fibers were employed as reinforcement: untreated wheat straw fibers (WSF) as a natural option and commercial polypropylene fibers (PPF) as a reference.

a Wheat Straw Fibers (WSF):

Wheat straw fibers were sourced from post-harvest residues in Constantine, Algeria. The straw fibers were obtained from dried straw stems and were manually cut using a sharp cutter in order to obtain fibers with an average length of approximately 20 mm (Figure 4). Due to the manual cutting process, a slight variability in fiber length was observed, estimated at approximately ±2 mm. Prior to use, the fibers were oven-dried at 60 °C for 48 h and stored in sealed polyethylene bags.

Figure 4. Natural and synthetic fibers used in this study: (**left**) polypropylene fibers (PPF) and (**right**) wheat straw fibers (WSF).

Physical properties, including bulk density, water absorption capacity, true density, and porosity, were determined following the procedures of RILEM TC 236-BBM [45] and Liuzzi et al. [46]. Table 4 summarizes the measured properties of straw.

Table 4. Properties of the wheat straw fibers (WSF).

Properties	Wheat Straw Fiber (WSF)
Bulk density (kg/m^3)	31.6 ± 3.1
True density (kg/m^3)	812.9 ± 11.8
Porosity (%)	96.11
Water content in the ambient atmosphere (%)	9 ± 0.65
Average diameter (mm)	1.6–3.0
Water absorption (%)	351 ± 23.5
Maximum tensile strength (MPa)	28.83 ± 7.61

b. Polypropylene Fibers (PPF):

The synthetic fibers used were polypropylene fibers (PPF) (TUF-STRAND MAXTEN), supplied by The Euclid Chemical, with a nominal length of 20 mm (Figure 4). The physical and mechanical properties, such as mass density and tensile strength, were provided by the manufacturer (see Table 5).

Table 5. Manufacturer-provided characteristics of polypropylene fibers (PPF).

Parameters	Value
Density (kg/m^3)	910 ± 5
The amount of polypropylene (%)	1.8–3.0 ± 0.2
Young's modulus (MPa)	3500–3900 ± 100
Tensile strength (MPa)	600–650 ± 25
Melting point (°C)	165 ± 2
Water absorption (%)	negligible

2.1.3. Design and Manufacturing of Samples

The dredged reservoir sediment (DRS) was oven-dried at 50 °C to constant mass, disaggregated using a mortar and pestle, and sieved through a 2 mm mesh. Fiber-reinforced mixtures were prepared using wheat straw fibers (WSF) and polypropylene fibers (PPF) at contents of 0%, 0.3%, 0.6%, and 0.9% by dry mass of sediment.

Fibers were first dry-mixed with DRS to ensure uniform dispersion within the matrix(see Figure 5) Tap water was then added to reach the optimum water content (OWC) determined from Standard Proctor compaction (NF P94-093 [47]). After mixing, each blend was sealed in airtight containers and conditioned for 24 h at laboratory temperature (≈23 ± 2 °C) to allow uniform moisture equilibration prior to compaction.

Figure 5. Preparation steps of the specimens.

Specimens were statically compacted to their respective maximum dry density (MDD) in accordance with NF P94-093 compaction parameters. Cylindrical specimens (50 mm diameter × 20 mm height) were prepared for one-dimensional consolidation testing, while prismatic specimens (60 mm × 60 mm × 20 mm) were prepared for direct shear testing.

2.2. Methods

The experimental methods adopted in this study were selected to address the key performance requirements of landfill liner materials, namely mechanical stability under stress, controlled compressibility, and low hydraulic conductivity, while accounting for the potential modifications induced by fiber reinforcement (see Figure 6).

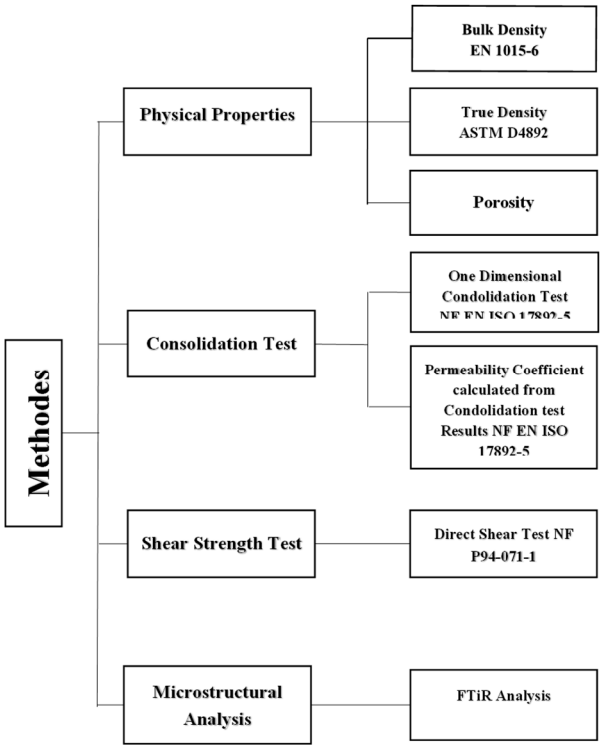

Figure 6. Schematic planning of the experimental plan followed in this work.

The shear strength behavior of fiber-reinforced DRS was evaluated using a controls-type direct shear box in accordance with NF P94-071-1 [48]. Prior to shear testing, Standard Proctor compaction tests were performed in accordance with NF P94-093 to determine the maximum dry density (MDD) and optimum moisture content (OMC) of both unreinforced and fiber-reinforced sediments. The sediment was tested without fibers and with varying fiber contents (0.3%, 0.6%, and 0.9%) using wheat straw fiber (WSF) and polypropylene fiber (PPF). The results of the Proctor tests were used to define the compaction parameters for the preparation of specimens for consolidation and shear testing. The obtained OMC values are presented in Table 6 and were used in specimen preparation.

Table 6. Mixture proportions of DRS-based composites.

Mixture ID	DRS (% Dry Mass)	WSF (% Dry Mass)	PPF (% Dry Mass)	Water Content (%)
DRS-0	100	0	0	14.80
DRS-WSF-0.3	99.7	0.3	–	14.89
DRS-WSF-0.6	99.4	0.6	–	14.91
DRS-WSF-0.9	99.1	0.9	–	15.79
DRS-PPF-0.3	99.7	–	0.3	14.80
DRS-PPF-0.6	99.4	–	0.6	14.80
DRS-PPF-0.9	99.1	–	0.9	14.80

Consolidated–drained direct shear tests were subsequently carried out under three normal stress levels (200, 300, and 400 kPa) at a constant horizontal displacement rate of 0.02 mm/min. Shearing was continued until a minimum horizontal displacement of 7 mm was reached. For each combination of fiber type (WSF or PPF), fiber content, and applied normal stress, three replicate tests were conducted to ensure the reliability and reproducibility of the results.

The bulk density (ρ_{bulk}) of compacted specimens was determined from mass and geometrical measurements using a precision scale and caliper. The true density (ρ_{true}) was measured using a helium gas pycnometer ULTRAPYC 1200-e (Quantachrome, Boynton Beach, FL, USA) in accordance with ASTM D4892 [49]. The total porosity (Φ) was calculated as:

$$\Phi = 1 - \frac{\rho_{bulk}}{\rho_{true}} \quad (1)$$

where Φ: is the total porosity in %, ρ_{bulk}: is the bulk density in kg/m^3 and ρ_{true}: is the true (apparent) density in kg/m^3.

One-dimensional consolidation tests were conducted to evaluate the compressibility and hydraulic behavior of both unreinforced and fiber-reinforced DRS. The tests were performed using a conventional oedometer apparatus in accordance with ISO 17892-5 [50]. The specimens were statically compacted into rigid rings with a diameter of 70 mm and a height of 20 mm.

The consolidation tests were carried out using a stepwise loading procedure. The applied vertical stress increments were 50, 100, 200, 400, and 800 kPa. Each load increment was maintained until the completion of primary consolidation before the subsequent load level was applied. Each loading step was sustained for 24 h to ensure the development of primary consolidation.

After reaching the maximum applied stress, unloading was performed in the reverse order of loading. Due to the time-consuming nature of the test, the consolidation experiments were repeated twice for each mixture to ensure the reliability of the results.

The hydraulic conductivity (k) of the DRS mixtures was indirectly estimated from consolidation parameters using the following relationship:

$$K = C_v * m_v * \gamma_w \quad (2)$$

C_v: coefficient of consolidation; m_v: coefficient of volume compressibility; γ_w = 10 kN/m^3.

To investigate potential physicochemical interactions between DRS and fibers, Fourier Transform Infrared Spectroscopy (FT-IR) analyses were performed using a JASCO FT/IR-4100 spectrophotometer(JASCO Inc., Tokyo, Japan). Samples were finely ground and scanned in transmission mode over the range 500–4000 cm^{-1}, with a spectral resolution of 2 cm^{-1}.

3. Results

3.1. Direct Shear Test

Figure 7 presents the Mohr–Coulomb failure envelopes for DRS specimens reinforced with different fiber contents. The corresponding shear strength parameters, cohesion (C), and internal friction angle (φ) are summarized in Table 7.

All tests were performed under identical conditions following standard direct shear procedures, with specimens compacted at OMC and MDD and tested under consolidated–drained conditions at normal stresses of 200, 300, and 400 kPa. For each configuration, three replicate tests were conducted, and the results are presented as mean values with associated standard deviations (Table 7), indicating limited variability and good repeatability.

The results indicate that fiber inclusion significantly modifies the shear strength behavior of the reinforced DRS. Up to an optimal fiber content of 0.6%, a general increase in the maximum shear stress (τ_{max}) was observed for both WSF- and PPF-reinforced specimens. This improvement can be attributed to the development of a reinforcing fiber network within the soil matrix, which enhances stress transfer and restricts particle displacement through frictional interlocking mechanisms [51].

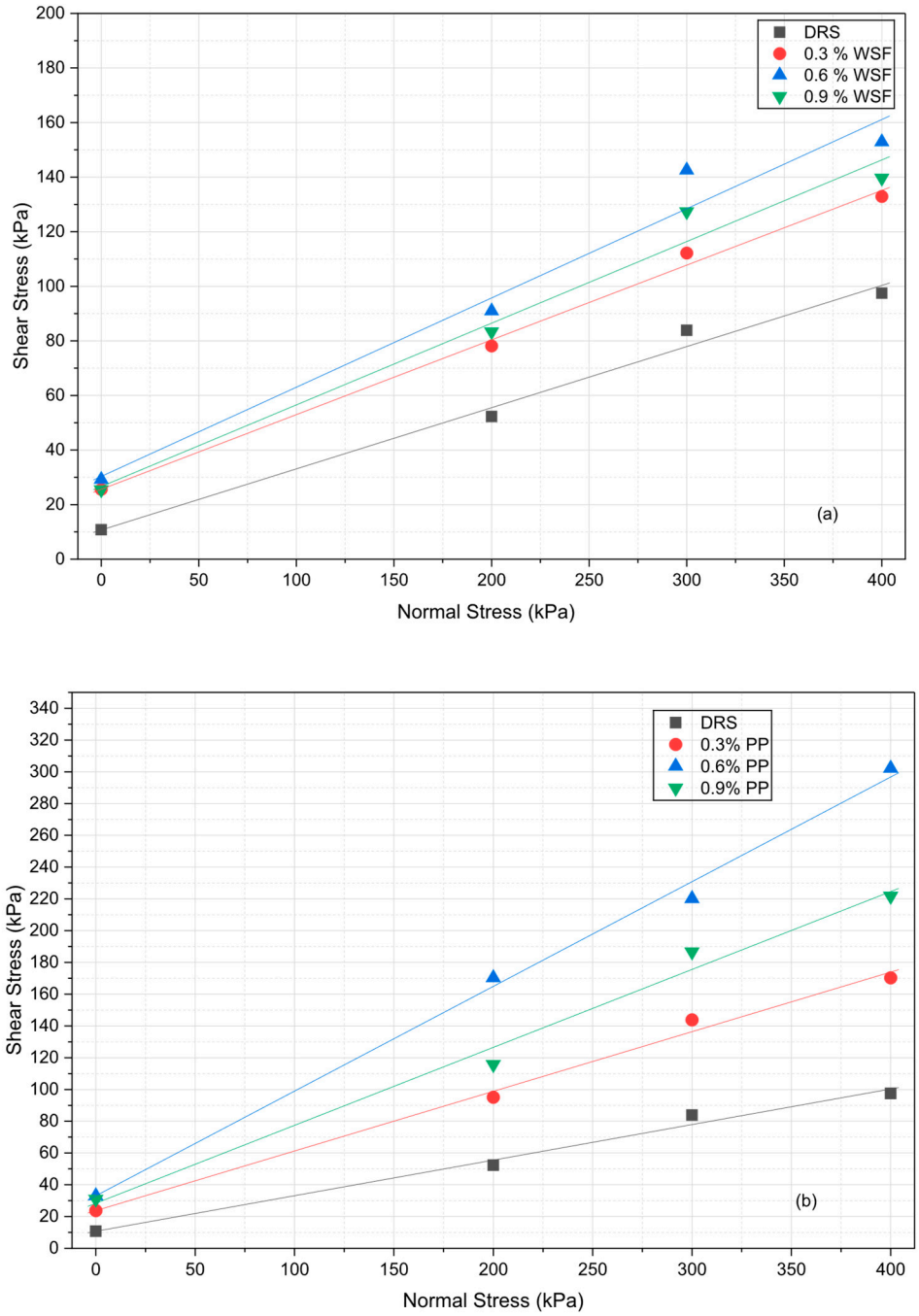

Figure 7. Mohr–Coulomb failure envelopes for fiber-reinforced and unreinforced DRS specimens: (**a**) WSF-reinforced DRS and (**b**) PPF-reinforced DRS.

Table 7. Variation in shear strength parameters with fiber content.

Fiber Content (%)	Apparent Cohesion C (kPa)	Friction Angle φ (°)
0% (DRS)	10.08 ± 1.22	17.53
0.3% WSF	24.59 ± 0.82	17.80
0.6% WSF	29.19 ± 1.11	18.77
0.9% WSF	26.47 ± 1.05	17.53
0.3% PPF	25.68 ± 2.10	25.97
0.6% PPF	32.99 ± 1.65	27.08
0.9% PPF	30.98 ± 0.07	26.51

However, beyond 0.6% fiber content (i.e., at 0.9%), a reduction in shear strength was observed, suggesting a threshold beyond which reinforcement efficiency decreases.

For WSF-reinforced specimens, the maximum shear stress under a normal stress of 200 kPa increased by approximately 73% at 0.6% fiber content compared to the unreinforced sample. At 0.9%, this increase declined to 58%. This reduction may be associated with limited mechanical stiffness and irregular geometry of straw fibers, which can reduce effective load transfer when fiber concentration becomes excessive.

Conversely, PPF demonstrated superior performance in enhancing shear strength. At 0.6% fiber content, the maximum shear stress increased to 170.25 kPa, representing an approximately 87% increase relative to WSF-reinforced DRS at the same fiber content. At 0.9%, shear strength decreased to 125.85 kPa, indicating that excessive fiber inclusion, even for synthetic fibers may reduce reinforcement efficiency due to fiber entanglement or non-uniform distribution within the matrix.

These results are consistent with previous studies reporting the existence of an optimal fiber dosage for maximizing mechanical performance in fine-grained soils [48]. Experimental evidence indicates that shear strength increases with fiber content up to a critical threshold, beyond which additional fibers may interfere with compaction, reduce dry density, decrease particle–particle contact, and promote clustering, ultimately disturbing matrix homogeneity. Similar behavior has been reported in cohesive soils, where peak strength is achieved at intermediate fiber contents, while higher dosages primarily improve ductility rather than peak load capacity [52].

The shear strength parameters derived from the Mohr–Coulomb envelopes are presented in Table 7. Both cohesion and internal friction angle increased with fiber content up to 0.6%, followed by a slight reduction at 0.9%, confirming a nonlinear response and the presence of an optimal fiber dosage.

For WSF reinforcement at 0.6%, cohesion increased to approximately 1.79 times that of unreinforced DRS, while the friction angle increased by a factor of 1.07. The relatively moderate increase in φ suggests that straw fibers primarily enhance apparent cohesion rather than frictional resistance.

PPF inclusion further enhanced shear strength parameters. At fiber contents of 0.3%, 0.6%, and 0.9%, cohesion values were 1.05, 1.13, and 1.17 times greater, respectively, than those of the corresponding WSF-reinforced specimens. The increase in friction angle was more pronounced, with ratios of 1.38, 1.90, and 1.54 relative to WSF mixtures at the same fiber contents. These results indicate that fiber type influences the balance between cohesion and frictional resistance, with PPF contributing more significantly to increases in internal friction.

The observed enhancement in shear strength may be attributed to two primary mechanisms: (i) increased frictional resistance resulting from fiber–soil interlocking and surface roughness effects [53], and (ii) an increase in apparent cohesion due to tensile resistance provided by fibers bridging potential failure planes [54,55].

3.2. Density and Porosity

Table 8 presents the bulk density and total porosity of unreinforced and fiber-reinforced DRS mixtures compacted at optimum water content. The unreinforced DRS exhibits a dry bulk density of 1.584 g/cm^3 and a corresponding porosity of 40.45%, values that are fully consistent with those reported for compacted fine-grained sediments and clayey soils used in liner applications. For instance, Marchiori et al. [56] reported dry bulk densities ranging from 1.50 to 1.65 g/cm^3 and porosities between 38 and 45% for water-treatment sludge-based compacted liners, while remaining compliant with hydraulic barrier requirements.

Table 8. Bulk and porosity of the DRS-based liner samples.

Sample	Bulk Density ρ_{bulk} (g/cm^3)	Porosity Φ (%)
DRS (0%)	1.584	40.45
0.3% WSF	1.570	40.58
0.6% WSF	1.555	40.74
0.9% WSF	1.535	41.11
0.3% PPF	1.580	40.26
0.6% PPF	1.560	40.68
0.9% PPF	1.545	40.91

The incorporation of wheat straw fibers (WSF) induces a gradual reduction in bulk density, from 1.570 g/cm^3 at 0.3% to 1.535 g/cm^3 at 0.9%, accompanied by a corresponding increase in porosity up to 41.11%. This trend reflects the lower intrinsic density of lignocellulosic fibers and their tendency to hinder particle rearrangement during compaction, leading to a more open soil fabric. Similar density reductions of 2–5% and porosity increases of ~1–3 percentage points have been reported for soils reinforced with natural fibers such as straw, coir, and jute at comparable dosages (0.25–1.0%) [35,57]. The slightly higher porosity observed at elevated WSF contents is consistent with the increased compressibility and permeability noted later, as excess fibers promote fiber clustering and localized voids within the matrix.

In contrast, polypropylene fiber (PPF) addition results in more limited changes in density and porosity. Bulk density remains close to that of the unreinforced DRS (1.580–1.545 g/cm^3), while porosity varies only marginally (40.26–40.91%). This behavior reflects the higher stiffness and smoother surface of PPF, which interferes less with particle packing during compaction. Comparable trends were reported by Plé and Lê [58], who observed density reductions below 2% in polypropylene-reinforced silty clays, with minimal changes in void structure. The restrained porosity increase explains the more favorable consolidation response and lower sensitivity of permeability observed for PPF-reinforced mixtures relative to WSF.

Overall, the density–porosity evolution confirms that fiber reinforcement does not compromise the compactability of DRS within the investigated range. The measured porosity values remain within the typical interval reported for compacted clay liners (35–45%) [3,5,56], ensuring adequate sealing capacity. The results further indicate that the optimum fiber content (≈0.6%) corresponds to a balance between mechanical reinforcement and limited alteration of the pore structure, whereas higher fiber contents primarily increase void ratio without proportional gains in performance.

3.3. Consolidation Test and Permeability Estimation

One-dimensional consolidation tests were conducted on DRS samples, both unreinforced and reinforced with WSF and PPF at fiber contents of 0.3%, 0.6%, and 0.9% (by dry mass of sediment), in order to evaluate the influence of fiber inclusion on key geotechnical parameters: the compression index (Cc), swelling index (Cs), coefficient of volume compressibility (mv), and coefficient of consolidation (Cv). The results are summarized in Table 9.

Overall, the incorporation of fibers led to a reduction in Cc, Cs, mv, and Cv up to an apparent optimal fiber content of 0.6%. At 0.9%, a slight increase in some parameters was observed for both fiber types, suggesting that excessive fiber content may reduce reinforcement efficiency due to dispersion limitations.

Table 9. Compressibility and consolidation results.

Material	Compression Index	Coefficient of Consolidation ($C_v \times 10^{-3}$: cm^2/s)	Coefficient of Volumetric Compressibility ($m_v \times 10^{-3}$: m^2/kN)	Swelling Index (C_s)
DRS	0.327	0.43	3.7	0.029
0.3% WSF	0.326	0.36	2.5	0.021
0.6% WSF	0.303	0.34	2.7	0.022
0.9% WSF	0.316	0.12	2.6	0.019
0.3% PPF	0.210	0.36	1.97	0.025
0.6% PPF	0.164	0.28	1.64	0.023
0.9% PPF	0.192	0.28	1.00	0.022

For WSF-reinforced samples, the compression index decreased from 0.327 to 0.303 at 0.6% fiber content (approximately 8% reduction), before increasing to 0.316 at 0.9%. This moderate improvement may be attributed to limited interfacial bonding and the relatively low stiffness of straw fibers within the DRS matrix.

In contrast, PPF was significantly more effective in reducing compressibility. At 0.6% fiber content, Cc decreased from 0.327 to 0.164, corresponding to an approximate 50% reduction. A slight increase to 0.192 at 0.9% was observed, likely due to reduced dispersion efficiency at higher fiber contents [59]. The marked reduction in compressibility at 0.6% PPF may be associated with improved stress transfer and fiber–matrix interaction mechanisms [60].

Overall, PPF demonstrated greater effectiveness than WSF in reducing compressibility, particularly at 0.6%. While wheat straw fibers offer environmental and economic advantages, their reinforcement efficiency appears limited beyond this dosage. Importantly, all C_c values remained within the typical range for compacted clays ($C_c < 0.5$), indicating acceptable consolidation behavior for liner applications [56].

Regarding the coefficient of consolidation (C_v), a general decrease was observed with increasing fiber content. For WSF-reinforced mixtures, C_v decreased notably at 0.9%, which may reflect increased structural heterogeneity and fiber clustering during mixing [38]. Changes in C_v are influenced by both permeability and compressibility, and therefore should be interpreted in conjunction with m_v and hydraulic conductivity values [39,61].

Concerning the swelling index (C_s), WSF-reinforced samples exhibited lower C_s values at 0.3% and 0.9% compared to DRS, although variations remained limited. The hydrophilic nature of straw fibers may contribute to localized water retention within the matrix. In contrast, C_s decreased progressively with increasing PPF content, from 0.029 (DRS) to 0.022 at 0.9% (≈24% reduction), indicating improved control of volumetric expansion. Similar trends have been reported by Muhammad et al. [61] and Viswanadham et al. (2009) [62].

Hydraulic conductivity is a critical parameter in the design of landfill cover and liner systems, as it governs fluid migration [3,56]. Typical design guidelines indicate values on the order of $\leq 1 \times 10^{-9}$ m/s for compacted clay liners and $\leq 1 \times 10^{-7}$ m/s for cover systems.

Permeability was estimated indirectly from oedometer test results using the classical relationship proposed by Olson and Daniel [63], and later applied by Mata and Ledesma, 2003 [64] and Quang and Chai, 2015 [65]. All permeability values are reported in cm/s; for comparison with regulatory requirements expressed in m/s, appropriate unit conversion

was performed. Hydraulic conductivity was calculated from the coefficient of consolidation (C_v) and the coefficient of volume compressibility (m_v).

Permeability values were determined under three loading ranges: 100–200 kPa, 200–400 kPa, and 400–800 kPa. The variation in hydraulic conductivity with fiber content is shown in Figures 8 and 9.

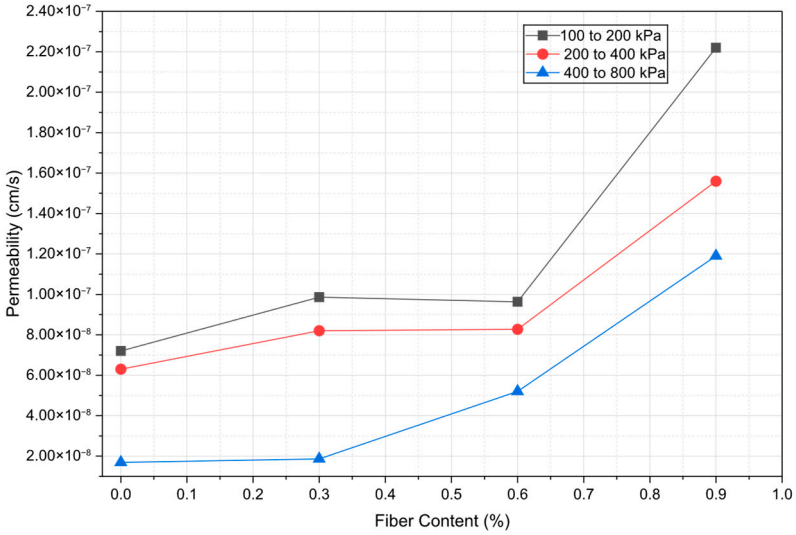

Figure 8. Hydraulic conductivity variations with WSF content at different loading steps.

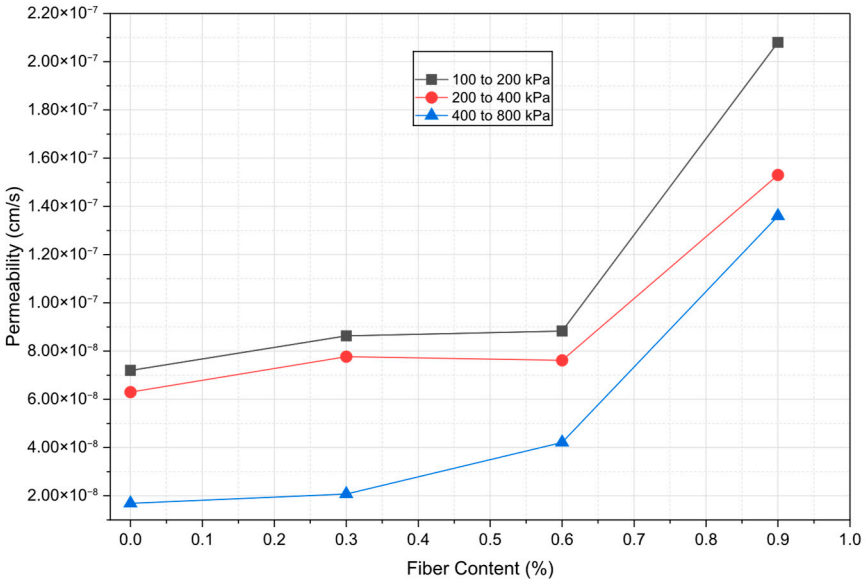

Figure 9. Hydraulic conductivity variations with PPF content at different loading steps.

An increase in fiber content from 0% to 0.9% resulted in a progressive increase in hydraulic conductivity. However, for fiber contents up to 0.3%, this increase remained marginal. For example, under the 400–800 kPa loading stage, permeability increased from 1.69×10^{-8} cm/s (DRS) to 1.86×10^{-8} cm/s (0.3% WSF) and 2.07×10^{-8} cm/s (0.3% PPF).

At 0.6% fiber content, hydraulic conductivity increased to 5.25×10^{-8} cm/s (WSF) and 4.21×10^{-8} cm/s (PPF), and at 0.9% to 1.19×10^{-7} cm/s (WSF) and 1.36×10^{-7} cm/s (PPF). The highest sensitivity was observed for 0.9% WSF under 100–200 kPa, where permeability reached 2.22×10^{-7} cm/s.

When converted to SI units, the highest measured permeability (1.36×10^{-7} cm/s) corresponds to 1.36×10^{-9} m/s, which remains two orders of magnitude lower than

the regulatory limit for landfill cover systems (10^{-7} m/s). Moreover, these values are substantially lower than the typical upper limits reported for compacted liner materials (Chaduvula et al., 2017 [66]; Divya et al., 2018 [67]), (Mukherjee and Mishra, 2019 [68]).

The increase in permeability can be attributed to the development of preferential flow paths induced by fiber inclusion (Mukherjee and Mishra, 2019 [68]), as was also reported by Muneerah et al., 2019 [39] Plé and Lê, 2012 [58], and Qiang et al., 2014 [69]). This interpretation is consistent with the measured increase in porosity (40.45% to 41.11% for WSF), indicating a slightly more open soil fabric.

Nevertheless, even at 0.9% fiber content, the estimated permeability (e.g., 1.36×10^{-7} cm/s for PPF) remains compatible with the hydraulic performance required for landfill cover systems. These results suggest that fiber reinforcement enhances mechanical stability without critically compromising the hydraulic barrier function.

3.4. Fourier Transform Infrared Spectroscopy (FT-IR)

The FTIR spectra of unreinforced and fiber-reinforced DRS (Figure 10) reveal the dominant mineralogical framework of the sediment and the progressive contribution of organic fibers with increasing dosage.

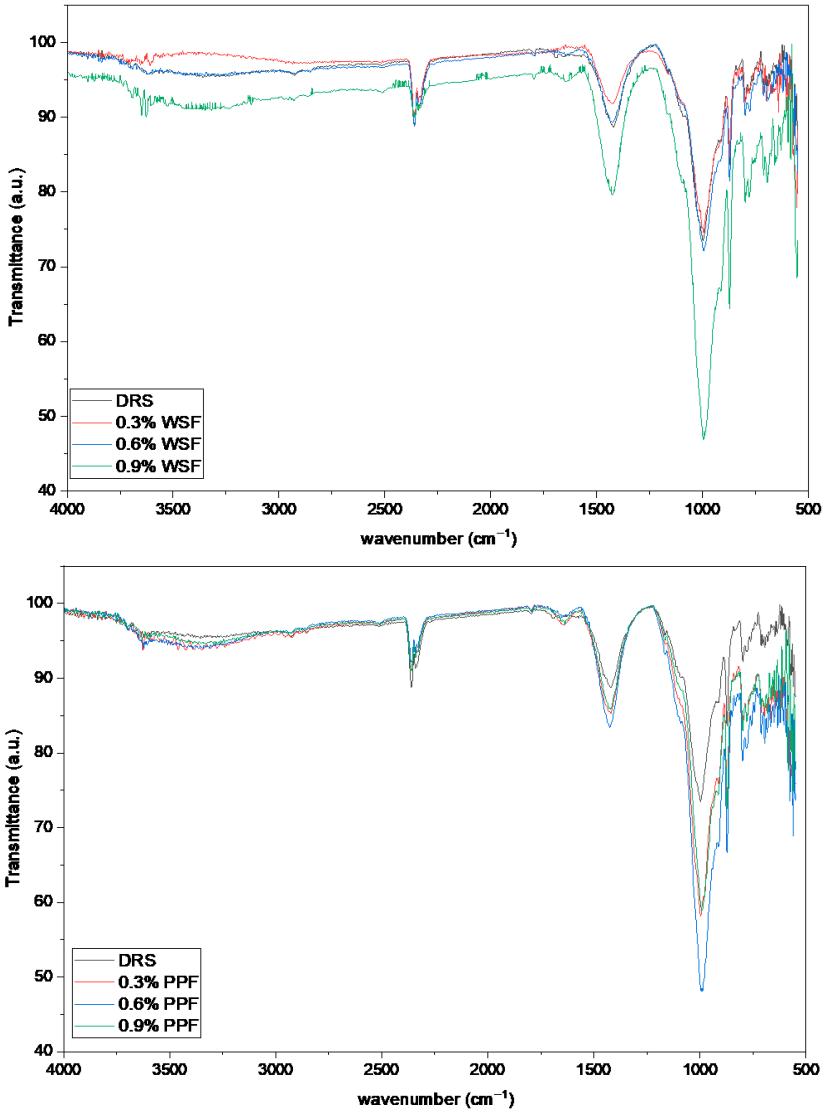

Figure 10. FTIR spectra of dam-extracted sediment (DRS) reinforced with wheat straw fibers (WSF) and polypropylene fibers (PPF) at different dosages.

All specimens exhibit a broad absorption band in the 3600–3200 cm^{-1} region, attributed to O–H stretching vibrations of structural hydroxyl groups in clay minerals together with physically adsorbed water. The band near 1640 cm^{-1} corresponds to H–O–H bending of the interlayer and adsorbed water molecules [70]. These features are typical of fine-grained clayey materials and reflect the hydrophilic nature of the mineral matrix, which governs compressibility and consolidation behavior.

A strong band centered at approximately 1030 cm^{-1} is assigned to Si–O stretching vibrations of aluminosilicate minerals [71], confirming the presence of clay minerals and quartz within the DRS. The persistence of this band across all mixtures indicates that fiber incorporation does not alter the fundamental mineral skeleton of the sediment. Secondary mineral-related bands, including those in the 520–470 cm^{-1} region, are consistent with Si–O–Al and Si–O–Si bending vibrations, further supporting the stability of the clay framework after reinforcement.

In WSF-reinforced mixtures, distinct organic signatures appear and intensify with increasing fiber content. The emergence of C–H stretching bands in the 2920–2850 cm^{-1} range is associated with aliphatic chains present in cellulose and hemicellulose. The band near 1730 cm^{-1} corresponds to C=O stretching vibrations of hemicellulosic ester groups [71], confirming the incorporation of lignocellulosic components.

Additional bands in the 1500–1600 cm^{-1} region are attributed to aromatic skeletal vibrations of lignin, which become more pronounced at higher WSF contents. Overlapping in the 1000–1100 cm^{-1} region between C–O–C and C–O vibrations of cellulose and Si–O stretching of clays results in slight band broadening, suggesting intimate physical contact between fibers and the clay matrix [72]. Importantly, no new absorption bands or peak shifts indicative of chemical bonding between mineral phases and organic fibers were observed. This suggests that the interaction between WSF and DRS is predominantly physical in nature, likely governed by frictional interlocking, hydrogen bonding, and mechanical bridging rather than chemical modification of the mineral structure.

The presence of hydrophilic hydroxyl and carbonyl functional groups in WSF may contribute to increased water affinity at the fiber–soil interface. This observation is consistent with the consolidation results, where moderate improvements in cohesion were accompanied by slight increases in compressibility and permeability at higher fiber contents.

In contrast, PPF-reinforced samples display only weak characteristic bands associated with polypropylene, primarily C–H stretching vibrations in the 2950–2840 cm^{-1} region and bending vibrations near 1455 and 1375 cm^{-1}. The absence of polar functional groups or additional oxygen-containing bands confirms the chemically inert nature of polypropylene.

No significant modification of clay-related bands was detected in PPF mixtures, indicating that the mineral matrix remains unaffected chemically. The reinforcement mechanism in PPF systems is therefore attributed primarily to mechanical interlocking and tensile resistance provided by the synthetic fibers.

Overall, the FTIR analysis confirms that fiber reinforcement does not induce chemical alteration of the DRS mineral structure. Instead, mechanical improvement arises from physical interaction mechanisms, with WSF introducing hydrophilic organic functionality and PPF acting as an inert structural inclusion.

4. Conclusions

This study investigated the feasibility of valorizing dredged reservoir sediments (DRS) as geomaterials for landfill liner and cover applications through fiber reinforcement. Particular emphasis was placed on the comparative evaluation of natural (wheat straw fibers, WSF) and synthetic (polypropylene fibers, PPF) reinforcements within the same

sediment matrix under liner-relevant conditions, providing new insight into their respective efficiencies and mechanisms.

- The unreinforced DRS exhibited properties compatible with liner applications, including high fines content (≈72%), moderate plasticity (PI ≈ 30), and porosity within the typical range of compacted clay materials (≈40%).
- Fiber inclusion significantly enhanced shear strength, with an optimal content of 0.6%. At this dosage, WSF increased shear strength by ≈73%, while PPF showed more pronounced and consistent improvements due to higher stiffness and more effective stress transfer. A reduction in performance beyond 0.6% indicates fiber oversaturation effects.
- Consolidation behavior improved with fiber addition, as reflected by a reduction in compressibility. The compression index decreased from 0.327 (DRS) to 0.303 (0.6% WSF) and 0.164 (0.6% PPF), confirming the effectiveness of reinforcement in limiting deformation.
- Hydraulic conductivity, indirectly estimated from consolidation parameters, showed a slight increase with fiber content but remained within ranges typically reported for compacted fine-grained barrier materials.
- Bulk density and porosity results indicated that fiber addition did not adversely affect compactability, with only marginal porosity increases (≈40.45% to 41.11%), remaining within acceptable limits.
- FTIR analysis highlighted distinct reinforcement mechanisms, with lignocellulosic interactions and increased water affinity for WSF, and mechanically driven reinforcement for PPF, confirming the influence of fiber nature on soil–fiber interaction.

Overall, this work demonstrates that DRS can be effectively reused as liner materials, while highlighting the distinct performance and mechanisms of natural and synthetic fibers within a unified experimental framework. The findings identify 0.6% fiber content as an optimal balance between mechanical improvement and material efficiency, with WSF offering a sustainable alternative despite lower performance compared to PPF. Future work should focus on direct permeability measurements and long-term durability assessment, as well as the evaluation of field-scale performance under realistic environmental conditions.

Author Contributions: Conceptualization, R.L., H.B., S.K. and A.B.; methodology, R.L., H.B., S.K. and A.B.; investigation, R.L. and H.B.; formal analysis, R.L., H.B., S.K. and A.B.; data curation, R.L. and H.B.; writing—original draft preparation, R.L. and H.B.; writing—review and editing, R.L., H.B., S.K. and A.B.; visualization, R.L., H.B., S.K. and A.B.; supervision, S.K. and H.B.; project administration, S.K. All authors have read and agreed to the published version of the manuscript.

Funding: This research received no external funding.

Institutional Review Board Statement: Not applicable.

Informed Consent Statement: Not applicable.

Data Availability Statement: The data presented in this study are available on request from the corresponding author due to privacy.

Conflicts of Interest: The authors declare no conflicts of interest.

References

1. Hamoda, M.F. Evaluation of landfill leachate in arid climate—A case study. *Environ. Int.* **2003**, *29*, 593–600. [CrossRef]
2. Yaqout, A.F.A.L.; Hamoda, M.F. Prediction of Contaminants Migration at Unlined Landfill Sites in an Arid Climate—A Case Study. *Water. Air. Soil Pollut.* **2005**, *162*, 247–264. [CrossRef]
3. Daniel, D.E. *Geotechnical Practice for Waste Disposal*; Chapman & Hall: London, UK, 1993.

4. Benson, B.C.H.; Member, A.; Zhai, H.; Wang, X. Estimating Hydraulic Conductivity of Compacted Clay Liners. *J. Geotech. Eng.* **1994**, *120*, 366–387. [CrossRef]
5. Row, R.K.E. Long-term performance of contaminant barrier systems. *Geotechnique* **2005**, *55*, 631–678. [CrossRef]
6. Mitchell, J.K.; Soga, K.; Wiley, J. *Fundamentals of Soil Behavior*; Wiley: Hoboken, NJ, USA, 2005.
7. Waheed, A.; Hafeez, I. Experimental development of clay liners for waste containment in arid and semi arid regions. *J. Chin. Inst. Eng.* **2018**, *41*, 687–696. [CrossRef]
8. Pits, A.B.; Factors, R.; Procedure, R. Abandoned Borrow Pits; Risk Factors and Reclamation Procedure. *MOJ Civ. Eng.* **2017**, *2*, 00033. [CrossRef]
9. Loudini, A.; Ibnoussina, M.; Witam, O.; Limam, A. Case Studies in Construction Materials Valorisation of dredged marine sediments for use as road material. *Case Stud. Constr. Mater.* **2020**, *13*, e00455. [CrossRef]
10. Amar, M.; Benzerzour, M.; Kleib, J.; Abriak, N.E. From dredged sediment to supplementary cementitious material: Characterization, treatment, and reuse. *Int. J. Sediment Res.* **2021**, *36*, 92–109. [CrossRef]
11. Hamouche, F.; Zentar, R. Effects of organic matter on mechanical properties of dredged sediments for beneficial use in road construction. *Environ. Technol.* **2018**, *41*, 296–308. [CrossRef]
12. Faiza, H.; Mohamed, M.; Gil, M.; Samir, T.; Rahmani, S.E.A. Erosion, Suspended Sediment Transport and Sedimentation on the Wadi Mina at the Sidi M'Hamed Ben Aouda Dam, Algeria. *Water* **2018**, *10*, 895. [CrossRef]
13. Boualem, R.; Wassila, H.; Des, R.; Versants, B. La sédimentation dans les barrages algériens. *La Houille Blanche* **2004**, *90*, 60–64. [CrossRef]
14. Bellara, S.; Maherzi, W.; Mezazigh, S.; Senouci, A.; Bellara, S.; Maherzi, W.; Mezazigh, S.; Senouci, A. Mineral waste valorization in road subgrade construction: Algerian case study based on technical and environmental features To cite this version: HAL Id: Hal-04495189 Case Studies in Construction Materials Algerian case study based on technical and environmental features. *Case Stud. Constr. Mater.* **2024**, *20*, e02764. [CrossRef]
15. Arjona, S.; Millares, A.; Baquerizo, A. Reservoir sedimentation impact downstream in a semi-arid basin with greenhouses cultivation. *E3S Web Conf.* **2018**, *40*, 03006. [CrossRef]
16. Maherzi, W.; Benzerzour, M.; Mamindy-pajany, Y.; Van, E. Beneficial reuse of Brest-Harbor (France) -dredged sediment as alternative material in road building: Laboratory investigations. *Environ. Technol.* **2017**, *39*, 566–580. [CrossRef]
17. Slag, B. Optimization of an Eco-Friendly Hydraulic Road Binders Comprising Clayey Dam Sediments and Ground Granulated. *Buildings* **2021**, *11*, 443. [CrossRef]
18. Maherzi, W.; Abdelghani, F. Ben Dredged Marine Raw Sediments Geotechnical Characterization for Their Reuse in Road Construction. *Eng. J.* **2014**, *18*, 27–37. [CrossRef]
19. Mkaouar, S.; Maherzi, W.; Pizette, P.; Zaitan, H.; Benzina, M. Journal of African Earth Sciences A comparative study of natural Tunisian clay types in the formulation of compacted earth blocks. *J. Afr. Earth Sci.* **2019**, *160*, 103620. [CrossRef]
20. Beddaa, H.; Ouazia, I.; Fraj, A.B.; Lavergne, F.; Torrenti, J.M. Reuse potential of dredged river sediments in concrete: Effect of sediment variability. *J. Clean. Prod.* **2021**, *265*, 121665. [CrossRef]
21. Hadj, R.; Belas, N.; Tahlaiti, M.; Mazouzi, R. Reusing calcined sediments from Chorfa II dam as partial replacement of cement for sustainable mortar production. *J. Build. Eng.* **2021**, *40*, 102273. [CrossRef]
22. Halassa, R.A.; Bibi, M.; Chikouche, M. Annales de Chimie—Science des Matériaux Behavior of Cementitious Materials under the Effect of an Eco-Cement Based on Dredged Sludge. *Ann. De Chim. Sci. Des Matériaux* **2021**, *45*, 455–465. [CrossRef]
23. Rozière, E.; Samara, M.; Loukili, A.; Damidot, D. Valorisation of sediments in self-consolidating concrete: Mix-design and microstructure. *Constr. Build. Mater.* **2015**, *81*, 1–10. [CrossRef]
24. Belayali, F.; Maherzi, W.; Benzerzour, M.; Abriak, N.; Senouci, A. Compressed Earth Blocks Using Sediments and Alkali-Activated Byproducts. *Sustainability* **2022**, *14*, 3158. [CrossRef]
25. Renella, G. Recycling and Reuse of Sediments in Agriculture: Where Is the Problem? *Sustainability* **2021**, *13*, 1648. [CrossRef]
26. Met, I.; Akgun, H. Geotechnical evaluation of Ankara clay as a compacted clay liner Geotechnical evaluation of Ankara clay as a compacted clay liner. *Environ. Earth Sci.* **2016**, *74*, 2991–3006. [CrossRef]
27. Teymur, B.; Dag, S.; Tolun, L.; Çevikbilen, G.; Bas, H.M.; Karadog, Ü. Assessment of the use of dredged marine materials in sanitary landfills: A case study from the Marmara sea. *Waste Manag.* **2020**, *113*, 70–79. [CrossRef]
28. Taylor, P.; Balkaya, M. Desalination and Water Treatment Evaluation of the use of alum sludge as hydraulic barrier layer and daily cover material in landfills: A finite element analysis study. *Desalination Water Treat.* **2015**, *57*, 2400–2412. [CrossRef]
29. Viswanath, S.M. Biopolymer Stabilised Earthen Construction Materials. Doctoral Thesis, Durham University, Durham, UK, 2019; pp. 1–194.
30. Al-soudany, K.Y.H.; Fattah, M.Y.; Rahil, F.H. Enhancement of Expansive Soil Properties by Water Treatment Sludge Ash in Landfill Liners. *Civ. Eng. J.* **2024**, *10*(no. 11), 3508–3530. [CrossRef]
31. Shukla, S.K. *Fundamentals of Fibre- Reinforced Soil Engineering*; Springer: Singapore, 2017.

32. Evangelou, E.D.; Markou, I.N.; Verykaki, S.E.; Bantralexis, K.E. *Mechanical Behavior of Fiber-Reinforced Soils under Undrained Triaxial Loading Conditions*; 2023; pp. 874–893.
33. Belhadad, H.; Bellel, N.; Bras, A. Influence of Alkali Treatment of Olive Husk on the Physical, Mechanical, and Hygrothermal Performance of a New Bio-Lightweight Concrete. In *Bio-Based Building Materials—Proceedings of ICBBM 2025*; RILEM Bookseries; Amziane, J., Filho, S.T., da Gloria, R.D., Page, M.Y.R., Eds.; Springer: Cham, Switzerland, 2025; Volume 61. [CrossRef]
34. Danso, H.; Martinson, D.B.; Ali, M.; Williams, J. Effect of fibre aspect ratio on mechanical properties of soil building blocks. *Constr. Build. Mater.* **2015**, *83*, 314–319. [CrossRef]
35. Zaimoglu, A.S.; Yetimoglu, T. Strength Behavior of Fine Grained Soil Reinforced with Randomly Distributed Polypropylene Fibers. *Geotech. Geol. Eng.* **2012**, *30*, 197–203. [CrossRef]
36. Sathishkumar, T.P.; Navaneethakrishnan, P.; Shankar, S.; Rajasekar, R.; Rajini, N. Characterization of natural fiber and composites—A review. *J. Reinf. Plast. Compos.* **2013**, *32*, 1457–1476. [CrossRef]
37. Alrshoudi, F.; Mohammadhosseini, H.; Alyousef, R.; Tahir, M.M.; Alabduljabbar, H.; Mohamed, A.M. The impact resistance and deformation performance of novel pre-packed aggregate concrete reinforced with waste polypropylene fibres. *Crystals* **2020**, *10*, 788. [CrossRef]
38. Qu, J.; Sun, Z. Strength Behavior of Shanghai Clayey Soil Reinforced with Wheat Straw Fibers. *Geotech. Geol. Eng.* **2015**, *34*, 515–527. [CrossRef]
39. Jeludin, M.; Suffri, N.; Rahim, S. The Consolidation Properties of Natural Fibre Clay Composite. In Proceedings of the 4th World Congress on Civil, Structural, and Environmental Engineering (CSEE'19), Rome, Italy, 1–9 April 2019. [CrossRef]
40. Belhadad, H.; Bellel, N.; Bras, A. Exploring the Dual Nature of Olive Husk: Fiber/Aggregate in Lightweight Bio-Concrete for Enhanced Hygrothermal, Mechanical, and Microstructural Properties. *Buildings* **2025**, *15*, 1950. [CrossRef]
41. *NF EN ISO 17892-4*; Geotechnical Investigation and Testing—Laboratory Testing of Soil—Part 4: Determination of Particle Size Distribution. AFNOR: La Plaine Saint-Denis, France, 2016.
42. *NF EN ISO 17892-3*; Geotechnical Investigation and Testing—Laboratory Testing of Soil—Part 3: Determination of Particle Density. AFNOR: La Plaine Saint-Denis, France, 2015.
43. *NF EN ISO 17892-12*; Geotechnical Investigation and Testing—Laboratory Testing of Soil—Part 12: Determination of Liquid and Plastic Limits. AFNOR: La Plaine Saint-Denis, France, 2018.
44. *NF EN ISO 10694*; Soil Quality—Determination of Organic and Total Carbon After Dry Combustion (Elementary Analysis). AFNOR: La Plaine Saint-Denis, France, 1995.
45. Amziane, S.; Collet, F.; Lawrence, M.; Magniont, C.; Picandet, V.; Sonebi, M. Recommendation of the RILEM TC 236-BBM: Characterisation testing of hemp shiv to determine the initial water content, water absorption, dry density, particle size distribution and thermal conductivity. *Mater. Struct. Constr.* **2017**, *50*, 67. [CrossRef]
46. Liuzzi, S.; Rubino, C.; Martellotta, F.; Stefanizzi, P.; Casavola, C.; Pappalettera, G. Characterization of biomass-based materials for building applications: The case of straw and olive tree waste. *Ind. Crop. Prod.* **2020**, *147*, 112229. [CrossRef]
47. *NF P 94-093*; Sols: Reconnaissance et Essais—Essai Proctor. AFNOR: La Plaine Saint-Denis, France, 2014.
48. *NF P 94-071-1*; Sols: Reconnaissance et Essais—Essai de Cisaillement à la boîte—Partie 1: Essai à la Boîte de Cisaillement. AFNOR: La Plaine Saint-Denis, France, 2011.
49. *ASTM D4892-14: 2019*; Standard Test Method for Density of Solid Pitch (Helium Pycnometer Method). ASTM International: West Conshohocken, PA, USA, 2019.
50. *NF EN ISO 17892-5*; Geotechnical Investigation and Testing—Laboratory Testing of Soil—Part 5: Incremental Loading Oedometer Test. AFNOR: La Plaine Saint-Denis, France, 2017.
51. Yu, X.; Wu, X.; Zhu, P.; Liu, C.; Qiu, C.; Cai, Z. Mechanism of Strength Degradation of Fiber-Reinforced Soil Under Freeze—Thaw Conditions. *Buildings* **2025**, *15*, 842. [CrossRef]
52. Patel, S.K.; Singh, B. Strength and Deformation Behavior of Fiber-Reinforced Cohesive Soil Under Varying Moisture and Compaction states. *Geotech. Geol. Eng.* **2017**, *35*, 1767–1781. [CrossRef]
53. Yetimoglu, T.; Salbas, O. A study on shear strength of sands reinforced with randomly distributed discrete fibers. *Geotext. Geomembr.* **2003**, *21*, 103–110. [CrossRef]
54. Kumar, A.; Walia, B.S.; Bajaj, A.; Stabilization, F.A. Influence of Fly Ash, Lime, and Polyester Fibers on Compaction and Strength Properties of Expansive Soil. *J. Mater. Civ. Eng.* **2007**, *19*, 242–248. [CrossRef]
55. Fonini, A.; Dalla, F.; Cesar, N. Geotextiles and Geomembranes Fiber reinforcement effects on sand considering a wide cementation range. *Geotext. Geomembr.* **2009**, *27*, 196–203. [CrossRef]
56. Marchiori, L.; Studart, A.; Albuquerque, A.; Pais, L.A.; Boscov, M.E.; Cavaleiro, V. Mechanical and Chemical Behaviour of Water Treatment Sludge and Soft Soil Mixtures for Liner Production Abstract. *Open Civ. Eng. J.* **2022**, *16*, e187414952211101. [CrossRef]
57. Attom, M.F.; Malkawi, A.I.H. Effect of fibres on the mechanical properties of clayey soil. *Proc. Inst. Civ. Eng.-Geotech. Eng.* **2009**, *162*, 277–282. [CrossRef]

58. Plé, O.; Lê, T.N.H. Effect of polypropylene fiber-reinforcement on the mechanical behavior of silty clay. *Geotext. Geomembr.* **2012**, *32*, 111–116. [CrossRef]
59. Al-kaream, K.W.A.; Fattah, M.Y.; Hameedi, M.K. Compressibility and strength development of soft soil by polypropylene fiber. *Geomate J.* **2022**, *22*, 91–97. [CrossRef]
60. Widianti, A.; Diana, W.; Bahti, F.N. Effect of fiber length on the consolidation parameters of coir fiber-reinforced soft clay. *E3S Web Conf.* **2023**, *429*, 04021. [CrossRef]
61. Ali, M.; Aziz, M.; Hamza, M.; Madni, M.F. Engineering properties of expansive soil treated with polypropylene fibers. *Geomech. Eng.* **2020**, *3*, 227–236.
62. Viswanadham, B.V.S.; Phanikumar, B.R.; Mukherjee, R. V Geotextiles and Geomembranes Swelling behaviour of a geofiber-reinforced expansive soil. *Geotext. Geomembr.* **2009**, *27*, 73–76. [CrossRef]
63. Ravichandran, N.; Krishnapillai, S. A Statistical Model for the Relative Hydraulic Conductivity of Water Phase in Unsaturated Soils. *Int. J. Geosci.* **2011**, *2011*, 484–492. [CrossRef]
64. Mata, C.; Ledesma, A. Permeability of a bentonite—Crushed granite rock mixture using different experimental techniques. *Geotechnique* **2003**, *53*, 747–758. [CrossRef]
65. Quang, N.D.; Chai, J.C. Permeability of lime- and cement-treated clayey soils. *Can. Geotech. J.* **2015**, *52*, 1221–1227. [CrossRef]
66. Chaduvula, U.; Viswanadham, B.V.S.; Kodikara, J. Applied Clay Science A study on desiccation cracking behavior of polyester fi ber-reinforced expansive clay. *Appl. Clay Sci.* **2017**, *142*, 163–172. [CrossRef]
67. Divya, P.V.; Viswanadham, B.V.S.; Gourc, J.P. Hydraulic conductivity behaviour of soil blended with geo fiber inclusions. *Geotext. Geomembranes* **2018**, *46*, 121–130. [CrossRef]
68. Mukherjee, K.; Mishra, A.K. Hydro-Mechanical Properties of Sand-Bentonite-Glass Fiber Composite for Landfill Application. *KSCE J. Civ. Eng.* **2019**, *23*, 4631–4640. [CrossRef]
69. Qiang, X.; Hai-jun, L.; Zhen-ze, L.; Lei, L. State Key Laboratory of Geomechanics and Geotechnical Engineering, Institute of Rock and Soil. *Eng. Geol.* **2014**, *178*, 82–90. [CrossRef]
70. Romano, A.; Grammatikos, S.; Riley, M.; Bras, A. Physicochemical characterisation of bio-based insulation to explain their hygrothermal behaviour. *Constr. Build. Mater.* **2020**, *258*, 120163. [CrossRef]
71. Ayeni, O.; Mahamat, A.A.; Bih, N.L.; Stanislas, T.T.; Isah, I.; Savastano Junior, H.; Boakye, E.; Onwualu, A.P. Effect of Coir Fiber Reinforcement on Properties of Metakaolin-Based Geopolymer Composite. *Appl. Sci.* **2022**, *12*, 5478. [CrossRef]
72. Madejová, J. FTIR techniques in clay mineral studies. *Vib. Spectrosc.* **2003**, *31*, 1–10. [CrossRef]